Desalination and Water Treatment
www.deswater.com

doi: 10.5004/dwt.2018.22010

108 (2018) 362–368
March

Synthesis, characterization and photodegradation application of Fe-Mn and F-MWCNTs supported Fe-Mn oxides nanoparticles

Khalid Saeed[a,b,*], Noor Zada[a], Idrees Khan[a], Muhammad Sadiq[a]

[a]*Department of Chemistry, University of Malakand, Chakdara, Dir (L), Khyber Pakhtunkhwa, Pakistan, Tel. +92 91 6540040; emails: khalidkhalil2002@yahoo.com (K. Saeed), syednoorzada88@gmail.com (N. Zada), idreeschem_uom@yahoo.com (I. Khan), sadiq@uom.edu.pk (M. Sadiq)*
[b]*Department of Chemistry, Bacha Khan University Charsadda, Khyber Pakhtunkhwa, Pakistan*

Received 2 August 2017; Accepted 8 February 2018

ABSTRACT

Multiwalled carbon nanotubes (MWCNTs) supported and unsupported bimetallic iron and manganese oxides nanoparticles (Fe-Mn NPs) were synthesized by wet chemical precipitation method. The synthesized nanoparticles were then characterized by various instrumental techniques such as scanning electron microscopy (SEM), energy dispersive X-ray and X-ray diffraction. The MWCNTs/Fe-Mn and Fe-Mn NPs were used as photocatalysts for the photodegradation of methylene blue in aqueous medium. The photodegradation study was monitored by using UV–Vis spectrophotometer. The effect of various parameters such as irradiation time, pH, catalyst dosage and concentration of dye on the photocatalytic degradation was studied. The activity of recovered catalyst was also examined.

Keywords: Multiwalled carbon nanotubes; Fe-Mn nanoparticles; Photodegradation; Methylene blue

1. Introduction

Photocatalysis is a simple technology for the chemical conversion of solar energy, during which a photoinduced reaction accelerated by the presence of a photocatalyst [1,2]. Photocatalysis has received great research interest due to its low cost, high efficiency and non-selective degradation [3]. This is an effective advance oxidation process and most emerging and promising technique successfully used for environmental remediation such as toxic and bioresistant pollutants in which semiconductor materials are used as a photocatalyst [4–6]. Photocatalyst is a semiconducting material activated by absorbing a photon having energy more than or equal to its band gap energy, and capability of accelerating photodegradation reaction without being consumed [7,8]. Such semiconductors are used to degrade organic pollutants in water to less toxic inorganic species and regenerate its chemical composition after reaction involvement [9,10]. Pollutants molecules get adsorbed on photocatalyst surface where chemical bond formation and breaking take place and as a result small molecules get released as products [5]. Currently, nanoparticles are used as photocatalysts due to their chemical stability, low photocorrosion, high surface area and uniform pore size [11]. Nanoparticles are small materials having at least one dimension less than 100 nm [12]. They attracted much attention as new materials due to their different physical and chemical properties from those of both bulk and atom [13]. Various metals and metals oxide nanoparticles were used as photocatalysts for the photodegradation of organic pollutants such as TiO_2 [14], Fe_3O_4 [15], Ag [16], Fe-doped ZnO [17], manganese-added ZnO hybrid nanoparticles [18], Mn-doped TiO_2 [19], etc. Currently, bimetallic nanoparticles and metal or nonmetal-doped metallic nanoparticles such as ZnS doped with Mn [20], TiO_2 loaded with Au (Au-TiO_2) [5], Ag-doped TiO_2 [21], etc., were also used as photocatalysts for photodegradation of organic pollutants. Nanoparticles tend to form strong agglomerates but in most applications such as photocatalysis, nanoparticles are required to be in a well-dispersed form, which require extremely high specific energy in order to overcome the adhesive forces [22].

* Corresponding author.

In the present study, bimetallic nanoparticles (neat Fe-Mn oxides NPs and multiwalled carbon nanotubes [MWCNTs]/Fe-Mn oxides NPs) were synthesized by wet chemical precipitation method. Both Fe-Mn oxides NPs and MWCNTs/Fe-Mn oxides NPs were used as photocatalysts for the photodegradation of methylene blue under UV light irradiation in aqueous medium. The effects of various parameters such as irradiation time, pH of the medium, catalyst dosage, dye concentration and recycled catalyst activity were also investigated.

2. Experimental

2.1. Materials

Iron chloride and manganese chloride ($MnCl_4$) were purchased from Scharlau (France) and Merck (Germany) companies, respectively, and used as received. The methylene blue was purchased from Sigma-Aldrich (Germany). Analytical grade nitric acid (HNO_3) and sulphuric acid (H_2SO_4) were purchased from Scharlau Company (France). The MWCNTs (diameter and length 20–40 nm and 30–40 μm, respectively) were supplied by Nanomirea (South Korea).

2.2. Functionalization of MWNTs

100 mL HNO_3 (6 M), 100 mL H_2SO_4 (2 M) and 0.5 g MWCNTs was taken in a flask and sonicated for 30 min. The mixture was refluxed at 170°C for 6 h and then cooled. The acid-treated MWCNTs were separated by filtration and then washed several times with distilled water in order to remove any attached acid from nanotubes. The MWCNTs were then dried in oven at 110°C and stored for further use.

2.3. Synthesis of Fe-Mn NPs

100 mL $FeCl_3$ (0.1 M) and 100 mL $MnCl_4$ (0.1 M) solutions was taken in round-bottom flask, and added NaOH (0.2 M) solution drop wise until the pH became basic. The mixture was then stirred continuously for 2 h at 60°C. The mixture was cooled and then the Fe-Mn oxides NPs were separated by filtration.

2.4. Synthesis of MWNTs/Fe-Mn NPs

100 mL $FeCl_3$ (0.1 M), 100 mL $MnCl_4$ (0.1 M) solutions and known quantity of F-MWCNTs were taken in round-bottom flask and then added NaOH (0.2 M) solution drop wise to the mixture at constant stirring until basic pH was obtained. The mixture was heated at 60°C for 2 h with occasional stirring. The mixture was cooled and then filtered to get the MWCNTs/Fe-Mn oxides NPs.

2.5. Photodegradation of MB dye using F-MWNTs/Fe-Mn and Fe-Mn NPs

0.0156 g F-MWNTs/Fe-Mn and 0.0135 g of Fe-Mn photocatalysts were added to 10 mL of MB (25 ppm) solutions in 50 mL beakers separately. The beakers were sealed with colorless plastic to allow light and to avoid dehydration. The samples were placed in dark for 20 min in order to establish adsorption/desorption equilibrium. The solution mixture was then placed under UV light (254 nm, 15 W) with constant stirring for a given specific irradiation time. After specific irradiation time, the catalyst was separated from the dye solution by centrifugation. The dye degradation study was performed by UV–Vis spectrophotometer. The percent degradation of MB in aqueous media was calculated by the following equation [23].

$$\text{Degradation rate } (\%) = \left(\frac{C_0 - C}{C_0}\right) \times 100 \quad (1)$$

$$\text{Degradation rate } (\%) = \left(\frac{A_0 - A}{A_0}\right) \times 100 \quad (2)$$

where C_o is the initial dye concentration, C is the dye concentration after UV irradiation, A_o shows initial absorbance and A shows the dye absorbance after UV irradiation.

2.6. Instrumentations

The morphological study was performed by SEM Model No. JEOL-JSM-5910; JEOL Company, Japan. The energy dispersive X-ray (EDX) study was performed by EDX spectrometer Model Inea 200, UK, Company Oxford. The photodegradation study was monitored by UV/VIS spectrophotometer (Shimadzu 160 A, Japan).

3. Results and discussion

3.1. Morphological study

3.1.1. SEM and EDX

Fig. 1 shows the SEM images of supported and unsupported bimetallic nanoparticles. Fig. 1(a) shows the SEM images of F-MWCNTs/Fe-Mn oxides nanoparticles. The micrographs presented that the bimetallic nanoparticles are spherical in shape and well dispersed on the surface of F-MWCNTs. While the unsupported bimetallic nanoparticles were mostly present in agglomerated form (Fig. 1(b)). The formation of Fe-Mn oxides nanoparticles was also confirmed by their EDX analyses. Fig. 2 shows the EDX spectra of supported and unsupported bimetallic nanoparticles. Fig. 2(a) shows peaks for carbon, which was due to the supported materials CNTs. The presence of oxygen peaks in the both figures conform the formation of oxides nanoparticles and functionalization of nanotubes.

3.1.2. FT-IR study

Fig. 3 presents the FT-IR spectra of F-MWCNTs/Fe-Mn and Fe-Mn nanoparticles. The spectra show prominent peaks at about 583 cm^{-1}, which might be due to the Fe-Mn nanoparticles [24]. The FT-IR spectrum of F-MWCNTs/Fe-Mn (Fig. 3(a)) show peak at about 1,618 cm^{-1}, which might be due to the stretching vibration of C=O [25]. The spectrum also presents peaks in the range of 1,236–1,055 cm^{-1}, which might occur due to the stretching vibration of C–O [26].

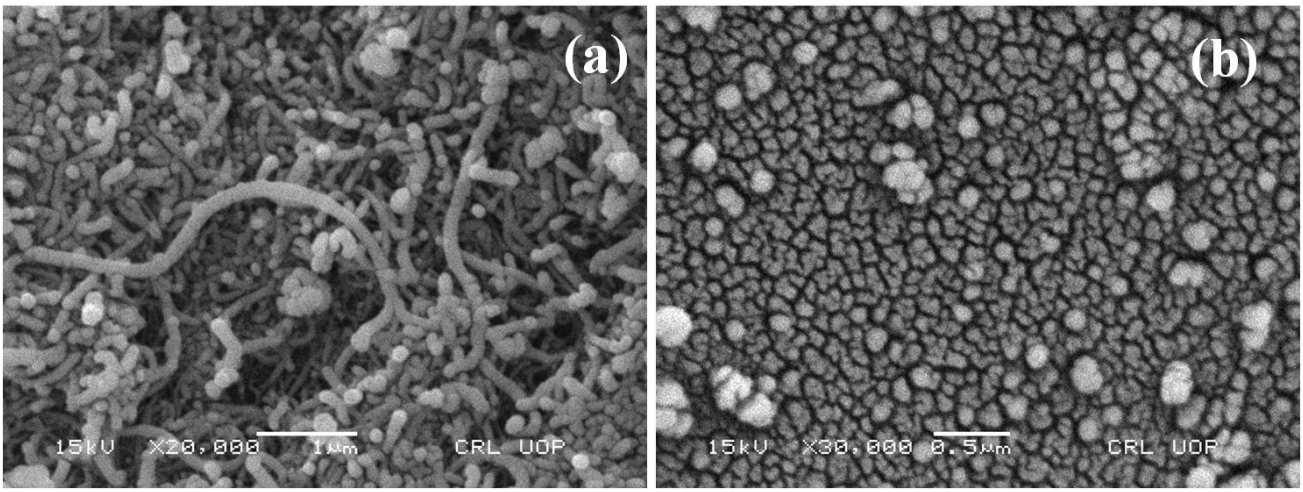

Fig. 1. SEM images of (a) FMWNTs/Fe-Mn nanoparticles and (b) unsupported Fe-Mn nanoparticles.

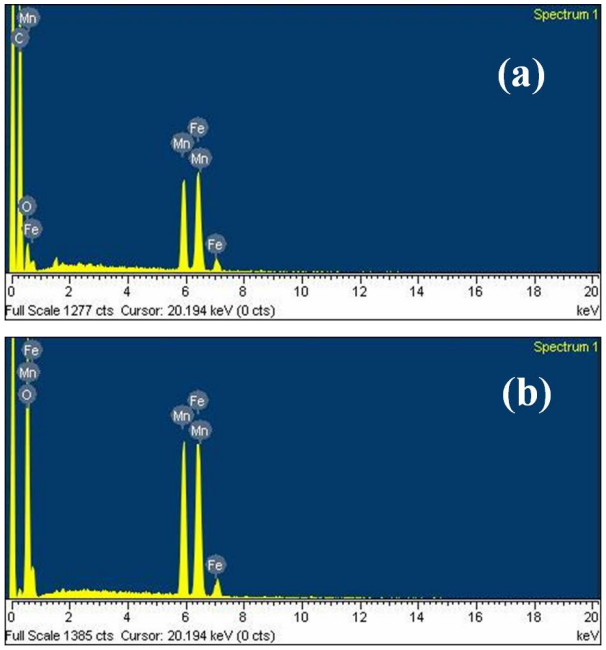

Fig. 2. EDX spectrum of (a) FMWNTs/Fe-Mn nanoparticles and (b) unsupported Fe-Mn nanoparticles.

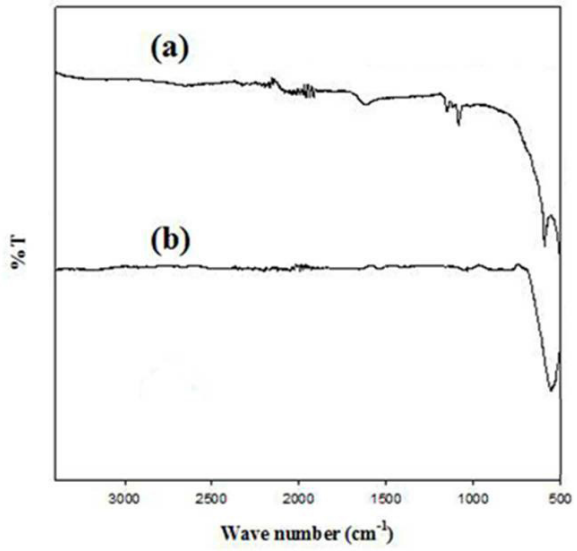

Fig. 3. FT-IR spectrum of (a) FMWNTs/Fe-Mn nanoparticles and (b) unsupported Fe-Mn nanoparticles.

Table 1
BET surface area and pore size of FMWNTs/Fe-Mn and Fe-Mn nanoparticles

Material name	BET surface area (m^2 g^{-1})	BJH pore volume (cc g^{-1})	BJH pore radius (Å)
Fe-Mn NPs	233.27	0.031	15.1
F-MWCNTs/ Fe-Mn	79.567	0.029	14.48

The pore size and surface area of F-MWCNTs/Fe-Mn and Fe-Mn nanoparticles are shown in Table 1. The pore size and surface area of the material was characterized by Quantachrome Nova version 11.04 (USA) surface area and pore size analyzer. Before adsorption the material was degassed at 400 K for 120 min in the presence of molecular nitrogen. The BET surface area of the material was found in the range of P/°P ~ 0.05–0.3. The surface area parameter of the material is described in Table 1.

3.1.3. Photodegradation study of methylene blue

Photocatalytic activity of synthesized F-MWCNTs/Fe-Mn and Fe-Mn oxides photocatalysts were studied by degrading MB dye in aqueous medium under UV light irradiation. MB is a basic dye and heterocyclic aromatic compound [27]. In this study, MB was chosen because it is used as a traditional dye and has many uses in the fields of biology and chemistry [28]. It produces burning sensation and may cause vomiting, nausea, diarrhea and gastritis if ingested, whereas it can lead to short periods of rapid or difficult breathing if inhaled [29].

Fig. 4 shows the UV–Vis spectra of MB in aqueous solution before and after UV irradiation in the presence of F-MWCNTs/Fe-Mn and Fe-Mn oxides NPs. The photodegradation of MB was measured by the relative intensity of its UV–Vis spectra, which gave maximum absorbance peak at 650 nm. The spectra presented that the photodegradation of MB gradually increased as the irradiation time increased. Fig. 3(c) shows the comparison of % degradation of MB dye photodegraded by supported and unsupported photocatalysts. The F-MWCNTs/Fe-Mn oxides NPs degraded 70% of dye within 2 h, while Fe-Mn oxides NPs photocatalysts degraded 65.5% of dye within the same period of time. At optimum time of 12 h, F-MWCNTs supported NPs and unsupported NPs degraded about 93.7% and 92.8% dye, respectively.

The photodegradation of dye can be achieved by the fact that when UV light falls upon the NPs, the valence electrons (e^-) of metal NPs get excited from valence band to conduction band, which create electron deficient or positive hole (h^+) in the valence band. The separated electrons and holes participate in the generation of reactive radicals. For example, the holes react with water molecules or hydroxide anions and generate hydroxyl radicals ($^\bullet OH$), whereas electrons react with O_2 results in the formation of superoxide radical ions ($^\bullet O_2^-$). These highly reactive radicals participate in the photodegradation of dye. The function of nanotubes is the dispersion of NPs in order to increase its surface area for photon absorption. The major reaction mechanism under sunlight irradiation is summarized in the following equations [7,30].

$$NPs \rightarrow NPs\ (h^+ + e^-) \quad (i)$$

$$O_2 + e^- \rightarrow {}^\bullet O_2^- \quad (ii)$$

$$H_2O + h^+ \rightarrow {}^\bullet OH \quad (iii)$$

$$Dye + {}^\bullet O_2^- \rightarrow Degradable\ products \quad (iv)$$

$$Dye + {}^\bullet OH \rightarrow Degradable\ products \quad (v)$$

The reaction mechanism can also be understood from the proposed scheme in Fig. 5.

The effect of recovered catalysts was also studied by using the recovered catalysts. The catalysts were washed several times with deionized water in order to remove any adsorbed dye and other attached byproducts and used under the same experimental conditions. Fig. 6(a) shows the comparison of % degradation of dye photodegraded by using recovered Fe-Mn oxides NPs photocatalysts three times. The results revealed that degradation for the 1st, 2nd and 3rd time by the recovered Fe-Mn photocatalyst was 92.8%, 88.4% and 85.5% dye within irradiation of 12 h. Similarly, Fig. 6(b) shows the comparison of % degradation of MB dye by recovered F-MWCNTs/Fe-Mn oxides photocatalyst. The results illustrate that recovered F-MWCNTs/Fe-Mn degraded 93.7%, 93.3% and 86.6% dye used in series three times. The results (Fig. 6) show that the recovered photocatalysts also significantly degraded MB in aqueous medium but show less activity as compared with the original photocatalysts. This decrease in the photocatalytic activity of the recovered catalysts might be attributed to the deposition of photo insensitive hydroxides on the photocatalysts surface, which block its active site [31].

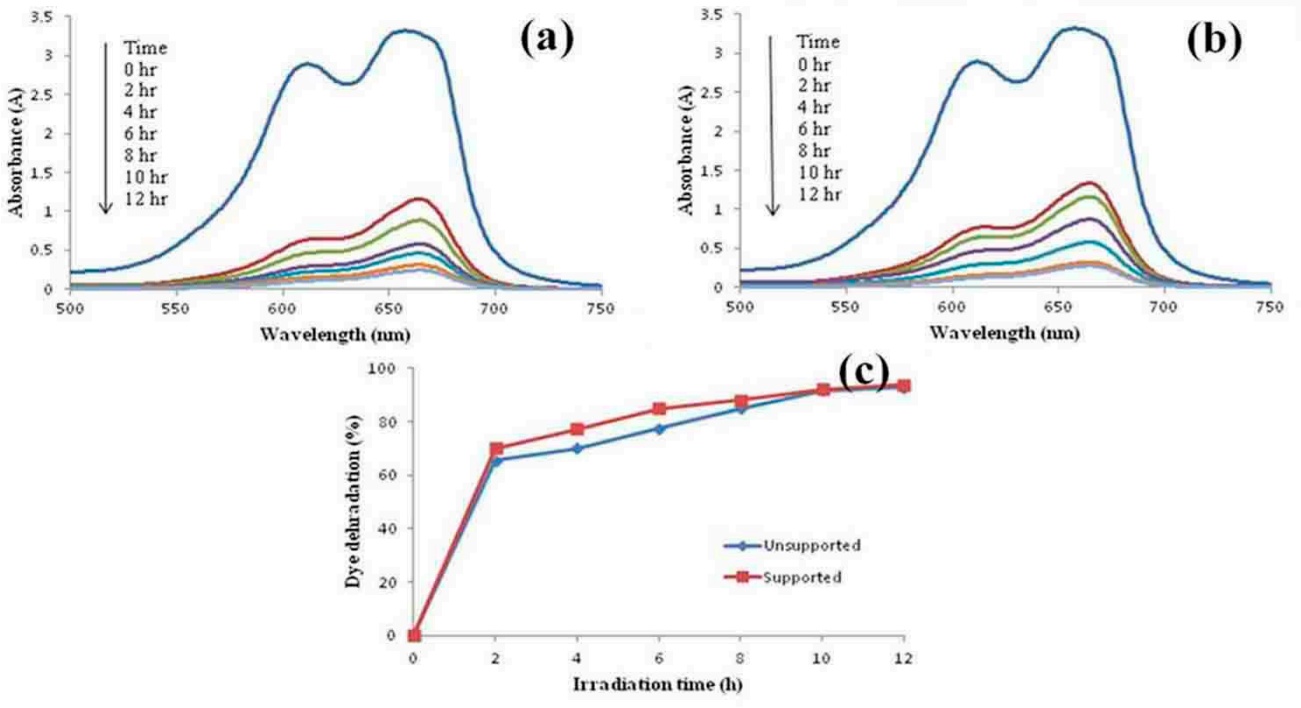

Fig. 4. UV–Vis spectra of methylene blue degraded by (a) F-MWCNTs/Fe-Mn nanoparticles, (b) Fe-Mn nanoparticles and (c) % degradation comparison.

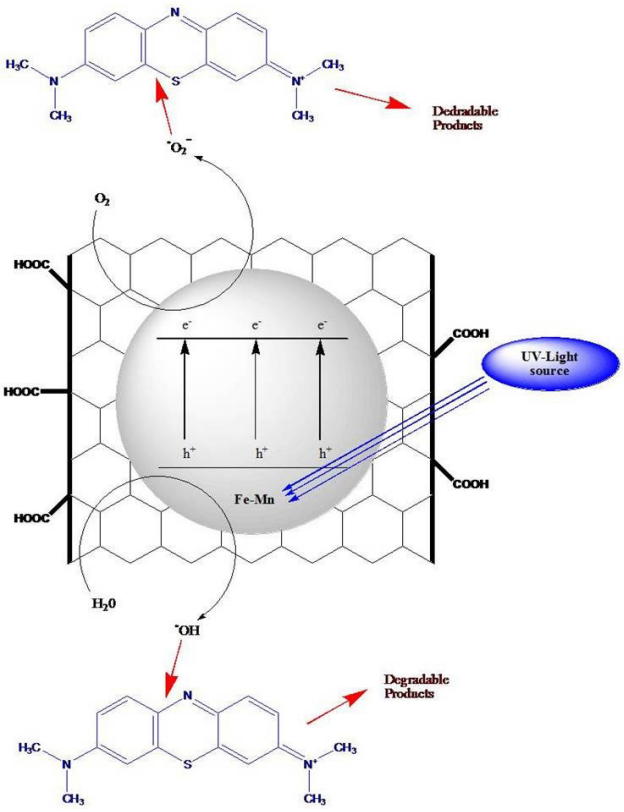

Fig. 5. Proposed mechanism for the photodegradation of methylene blue in aqueous medium.

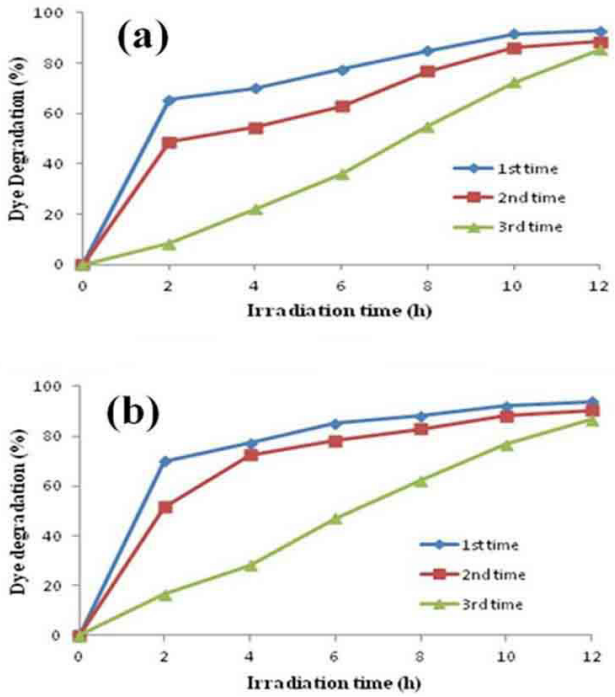

Fig. 6. % degradation comparison of methylene blue in aqueous medium (a) Fe-Mn nanoparticles and (b) F-MWCNTs/Fe-Mn nanoparticles.

4. Effect of pH of medium

Various industries such as paint, dyes, textile, surface coating, etc., discharge their effluents at different pH levels; therefore, the study of pH effect is also important. The effect of pH on photodegradation of MB is shown in Fig. 7. Fig. 7 shows the UV–Vis spectra and %degradation of MB in aqueous medium before and after UV light irradiation in the presence of F-MWCNTs/Fe-Mn and Fe-Mn oxides NPs. The results revealed that the F-MWCNTs/Fe-Mn oxides degraded about 77.2% dye at pH 4, which was gradually increased as increased the pH of the medium and at pH 10 about 95.5% of dye degraded within 8 h of irradiation time. Similarly, Fe-Mn oxides NPs degraded 41.7% at pH 4 and 92.9% at pH 10 under the same irradiation time. The higher photodegradation rate in the basic medium might be due to the enhanced formation of hydroxyl radicals and strong oxidizing species, which are responsible for higher degradation [23].

5. Effect of photocatalyst dosage

The effect of photocatalyst dosage on the photodegradation rate of the MB dye was studied by employing different catalyst quantity varying from 0.007 to 0.021 g per 10 mL dye solution at constant time (1 h). Fig. 8 shows the UV–Vis spectra and % degradation of MB dye before and after UV light irradiation employing different amounts of F-MWCNTs/Fe-Mn and Fe-Mn oxides NPs, respectively. Fig. 8(c) shows the comparison of MB dye by both supported and unsupported photocatalysts. The results (Fig. 7(c)) show that 0.007 g of both supported and unsupported catalysts degraded about 79.2% and 62.2% dye, respectively. The gradual increasing of % decolorization was observed as the catalyst amount increases, and by adding 0.021 g of F-MWCNTs/Fe-Mn and Fe-Mn oxides NPs degraded about 86.7% and 84.4%, respectively, within the same irradiation time.

6. Effect of initial dye concentration

The effect of initial dye concentration on degradation efficiency was monitored by studying the photocatalysis process at various dye concentrations (20, 30, 40, 50, 60 and 70 ppm). Fig. 9 shows the % degradation of dye at various dye concentration using constant catalyst dosage and irradiation time. The results revealed that the photodegradation of dye decreases gradually as the initial concentration of dye increased. The observed decrease might be due to the increased dye concentration because as the dye molecules adsorbed on catalyst surface which absorb significant amount of UV light rather than bimetallic nanoparticles. Also due to the high dye concentration, the formation of hydroxyl radicals decreased because of dye molecules, which occupy active sites of photocatalyst [32]. It was also found that the supported and unsupported bimetallic NPs degraded about 90% and 85% dye at initial dye concentration of 20 ppm, and 39% and 36% dye at 70 ppm.

7. Conclusion

Functionalization of MWCNTs improves its interaction with prepared bimetallic nanoparticles. F-MWCNTs supported and unsupported Fe-Mn oxides nanoparticles were

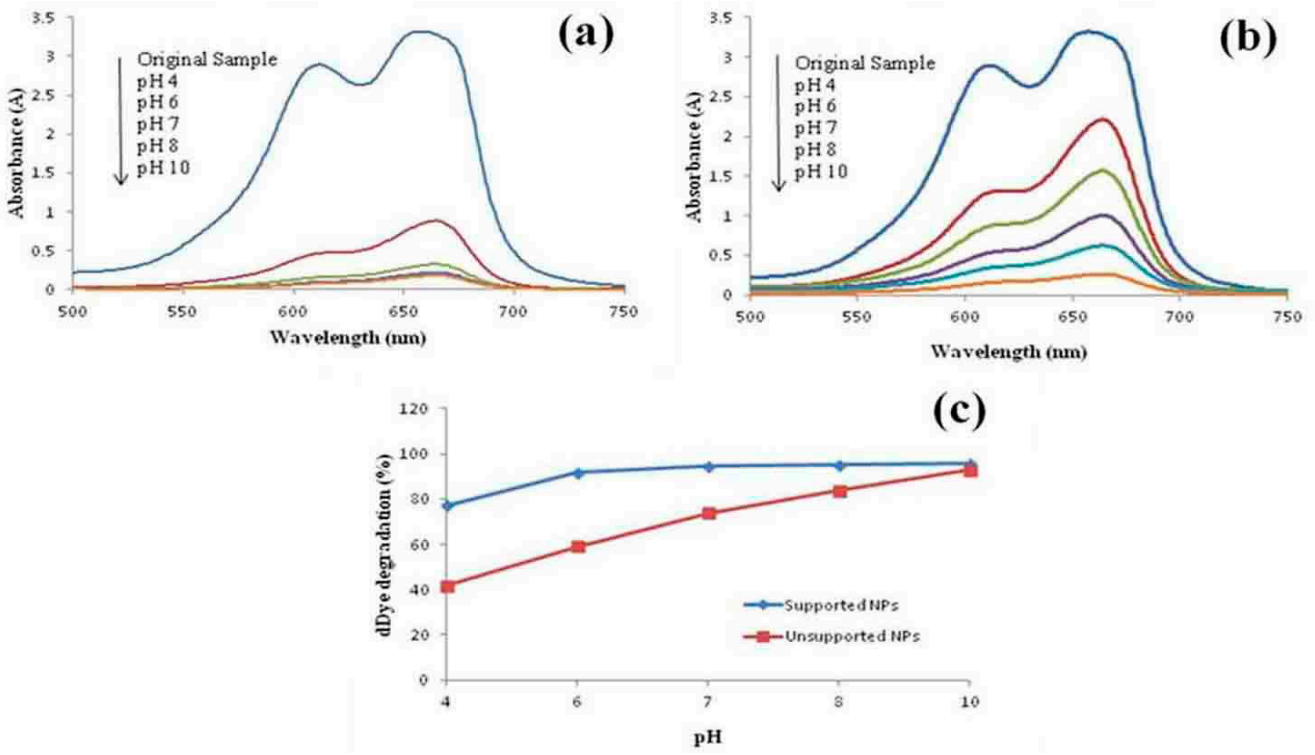

Fig. 7. UV–Vis spectra of methylene blue at different pH by (a) Fe-Mn nanoparticles, (b) F-MWCNTs/Fe-Mn nanoparticles and (c) comparison of % degradation at different pH by supported and unsupported Fe-Mn photocatalysts.

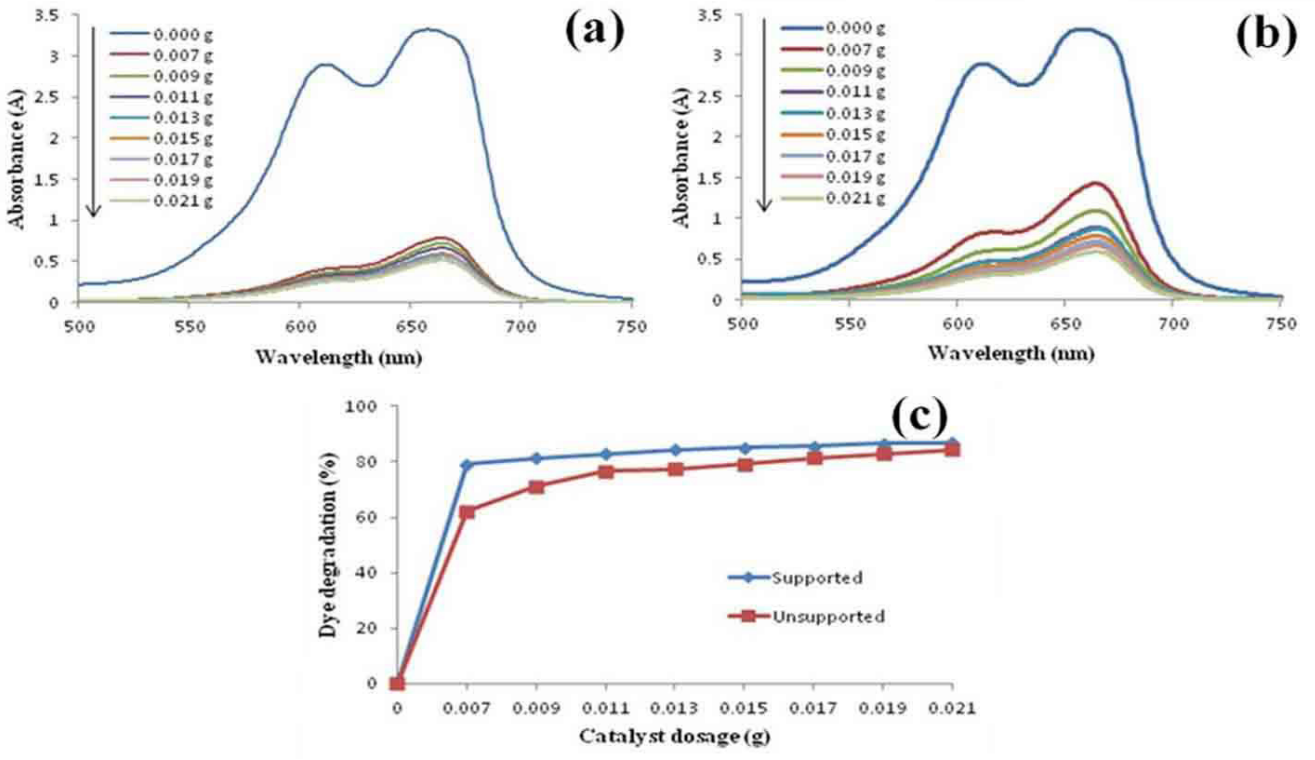

Fig. 8. UV–Vis spectra of methylene blue at various amounts of (a) F-MWCNTs/Fe-Mn, (b) Fe-Mn nanoparticles and (c) % degradation comparison.

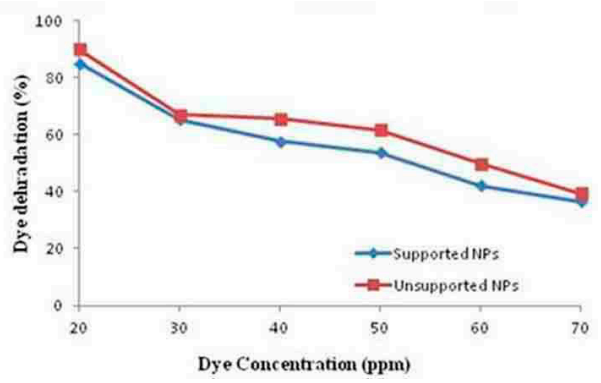

Fig. 9. Effect of F-MWCNTs/Fe-Mn and Fe-Mn at different dye concentration.

used as a photocatalysts for the photodegradation of MB and it was found that F-MWCNTs/Fe-Mn oxides NPs is more efficient than unsupported Fe-Mn oxides NPs. The photodegradation study of recovered and re-covered catalysts presented that both had ability to degrade the MB in aqueous medium but show less activity as compared with fresh catalysts. The photodegradation rate was found higher in basic medium and at low initial dye concentration.

References

[1] U.G. Akpan, B.H. Hameed, Parameters affecting the photocatalytic degradation of dyes using TiO_2-based photocatalysts: a review, J. Hazard. Mater., 170 (2009) 520–529.
[2] D. Ayodhya, M. Venkatesham, A.S. Kumari, G.B. Reddy, D. Ramakrishna, G. Veerabhadram, Photocatalytic degradation of dye pollutants under solar, visible and UV lights using green synthesized CuS nanoparticles, J. Exp. Nanosci., 11 (2016) 418–432.
[3] A. Mohamed, R. El-Sayed, T.A. Osman, M.S. Toprak, M. Muhammed, A. Uheida, Composite nanofibers for highly efficient photocatalytic degradation of organic dyes from contaminated water, Environ. Res., 145 (2016) 18–25.
[4] R.D.C. Soltani, Z. Haghighat, Visible light photocatalysis of a textile dye over ZnO nanostructures covered on natural diatomite, Turk. J. Chem., 40 (2016) 454–466.
[5] P.S.S. Kumar, R. Sivakumar, S. Anandan, J. Madhavan, P. Maruthamuthu, M. Ashokkumar, Photocatalytic degradation of acid red 88 using Au–TiO_2 nanoparticles in aqueous solutions, Water Res., 42 (2008) 4878–4884.
[6] B. Shahmoradi, A. Maleki, K. Byrappa, Removal of Disperse Orange 25 using in situ surface-modified iron-doped TiO_2 nanoparticles, Desal. Wat. Treat., 53 (2015) 3615–3622.
[7] K. Saeed, I. Khan, M. Sadiq, Synthesis of graphene-supported bimetallic nanoparticles for the sunlight photodegradation of Basic Green 5 dye in aqueous medium, Sep. Sci. Technol., 57 (2016) 1421–1426.
[8] M. Fox, Photocatalytic Oxidation of Organic Substances, M. Schiavello, Ed., Photocatalysis and Environment: Trends and Applications, New York Academic Publishers, New York, 1988.
[9] O. Sharma, M.K. Sharma, Copper hexacyanoferrate(II) as photocatalyst: decolorisation of neutral red dye, Int. J. ChemTech. Res., 5 (2013) 2706–2716.
[10] N. Serpone, A.V. Emeline, Suggested terms and definitions in photocatalysis and radiocatalysis, Int. J. Photoenergy, 4 (2002) 91–131.
[11] H.R. Pouretedal, M. Kiyani, Photodegradation of 2-nitrophenol catalyzed by CoO, CoS and CoO/CoS nanoparticles, J. Iran. Chem. Soc., 11 (2014) 271–277.
[12] C. Brochot, G. Mouret, N. Michielsen, S. Chazelet, D. Thomas, Penetration of nanoparticles in 5 nm to 400 nm size range through two selected fibrous media, J. Phys. Conf. Ser., 304 (2011) 1–9.
[13] M. Iwamoto, K. Kuroda, V. Zaporojtchenko, S. Hayashi, F. Faupel, Production of gold nanoparticles-polymer composite by quite simple method, Eur. Phys. J., 24 (2003) 365–367.
[14] M.H. Zori, Synthesis of TiO_2 nanoparticles by microemulsion/heat treated method and photodegradation of methylene blue, J. Inorg. Organomet. Polym. Mater., 21 (2011) 81–90.
[15] R.V. Solomon, I.S. Lydia, J.P. Merlin, P. Venuvanalingam, Enhanced photocatalytic degradation of azo dyes using nano Fe_3O_4, J. Iran. Chem. Soc., 9 (2012) 101–109.
[16] G.G. Selvam, K. Sivakumar, Phycosynthesis of silver nanoparticles and photocatalytic degradation of methyl orange dye using silver (Ag) nanoparticles synthesized from *Hypnea musciformis* (Wulfen) J.V. Lamouroux, Appl. Nanosci., 5 (2015) 617–622.
[17] A. Maleki, B. Shahmoradi, Solar degradation of Direct Blue 71 using surface modified iron doped ZnO hybrid nanomaterials, Water Sci. Technol., 65 (2012) 1923–1928.
[18] B. Shahmoradi, K. Namratha, K. Byrappa, K. Soga, S. Ananda, R. Somashekar, Enhancement of the photocatalytic activity of modified ZnO nanoparticles with manganese additive, Res. Chem. Intermed., 37 (2011) 329–340.
[19] B. Shahmoradi, M. Negahdary, A. Maleki, Hydrothermal synthesis of surface-modified, manganese-doped TiO_2 nanoparticles for photodegradation of methylene blue, Environ. Eng. Sci., 29 (2012) 1032–1037.
[20] J.V. Tolia, M. Chakraborty, Z.V.P. Murthy, Photocatalytic degradation of malachite green dye using doped and undoped ZnS nanoparticles, Pol. J. Chem. Technol., 14 (2012) 16–21.
[21] C. Sahoo, A.K. Gupta, I.M.S. Pillai, Photocatalytic degradation of methylene blue dye from aqueous solution using silver ion-doped TiO_2 and its application to the degradation of real textile wastewater, J. Environ. Sci. Health A, 47 (2012) 1428–1438.
[22] C. Sauter, M.A. Emin, H.P. Schuchmann, S. Tavman, Influence of hydrostatic pressure and sound amplitude on the ultrasound induced dispersion and de-agglomeration of nanoparticles, Ultrason. Sonochem., 15 (2008) 517–523.
[23] K. Saeed, I. Khan, S.Y. Park, TiO_2/amidoxime-modified polyacrylonitrile nanofibers and its application for the photodegradation of methyl blue in aqueous medium, Desal. Wat. Treat., 54 (2015) 3146–3151.
[24] S.W. Hwang, A. Umar, G.N. Dar, S.H. Kim, R.I. Badran, Synthesis and characterization of iron oxide nanoparticles for phenyl hydrazine, Sensor Appl., 12 (2014) 1–5.
[25] M.S. Tehrani, P.A. Azar, P.E. Namin, S.M. Dehaghi, Removal of lead ions from wastewater using functionalized multiwalled carbon nanotubes with tris(2-aminoethyl)amine, J. Environ. Protect., 4 (2013) 529–536.
[26] V.H. Nguyenand, J.-J. Shim, Green synthesis and characterization of carbon nanotubes/polyaniline nanocomposites, J. Spectro., 2015 (2015) 1–9.
[27] V.S. Shrivastava, Photocatalytic degradation of methylene blue dye and chromium metal from wastewater using nanocrystalline TiO_2 semiconductor, Arch. Appl. Sci. Res., 4 (2012) 1244–1254.
[28] K. Dai, L. Lu, G. Dawson, Development of UV-LED/TiO_2 device and their application for photocatalytic degradation of methylene blue, JMEPEG, 22 (2013) 1035–1040.
[29] T.W. Kim, M.J. Lee, Effect of pH and temperature for photocatalytic degradation of organic compound on carbon-coated TiO_2, J. Adv. Eng. Technol., 3 (2010) 193–198.
[30] S. Tabasideh, A. Maleki, B. Shahmoradi, E. Ghahremani, G. McKay, Sonophotocatalytic degradation of diazinon in aqueous solution using iron-doped TiO_2 nanoparticles, Sep. Purif. Technol., 189 (2017) 186–192.
[31] S.T. Ong, W.S. Cheong, Y.T. Hung, Photodegradation of Commercial Dye, Methylene Blue Using Immobilized TiO_2, 4th International Conference on Chemical, Biological and Environmental Engineering, Vol. 43, 2012, pp. 109–113.
[32] K.M. Reza, A.S.W. Kurny, F. Gulshan, Parameters affecting the photocatalytic degradation of dyes using TiO_2: a review, Appl. Water Sci., 7 (2015) 1569–1578.